LQG CONTROL OF STEAM TEMPERATURE IN POWER PLANTS

Benoît Codrons

Laborelec s.c.r.l., Rodestraat 125, B-1630 Linkebeek, Belgium — benoit.codrons@laborelec.com — fax: +32 2 382 02 41

Keywords: Process control, LQG control, power plant, superheater, economics.

Abstract

This paper presents an application of LQG control to the regulation of steam temperature in a power plant. The (simulation) results are compared to those obtained with optimised PID controllers, and it is shown that LQG yields much tighter setpoint control especially during transients. It is shown that these improved control performance have significant positive economic repercussions.

1 Introduction

The ever-increasing economic pressure caused by deregulation of the European energy market has led to major changes in the way power plants are operated. They are faced with the need to become more and more flexible to fulfil load requirements imposed by the control of the electrical grid frequency; start-up times have to be reduced to a minimum; faster and more frequent load changes are imposed... This can be a real challenge from the control design point of view. More and more performant control structures are the price to be payed in order to reach the required level of flexibility without impairing the life of the equipment. It is indeed during load changes that power plants have to face the largest temperature and pressure transients, the amplitudes and gradients of which are an important cause of material stress and wear.

As is the case in most industrial sectors, PID control has always been favoured, essentially for its implementational advantages. It is however well known that the performance of PID controllers is often very limited when they are applied to systems of order larger than one or two and/or with important dead times and/or with strong interactions. In such cases, optimal control methods should be prefered. Doubtless, they will eventually permeate most industrial sectors; yet, nowadays, their applications in power generation are scarce. Some examples can be found in [4, 8, 9] and references therein.

The goal of this paper is to present the advantages of modern multivariable control techniques for the electricity sector, both from a technical and an economic point of view. We have therefore applied Linear Quadratic Gaussian design to one of the most critical loops encountered in a power plant: that of superheated steam temperature control. The tests have been carried out on a nonlinear realistic simulator, based on first-principles modelling, of a coal-fired 300 MW power plant.

2 Description of the process

The simulator used in this study is that of a 300 MW coal-fired power plant [3]. It is based on physical modelling and is valid in the entire load range. The language used for its programming is Cogito NT, which has been developed by Cegelec in Charleroi, Belgium, and is normally used to program control systems. The simulator features in particular the model of the thermo-hydraulic part of the process and all its control loops.

The boiler is a drum boiler with six superheaters in two parallel series. As both series are identical and controlled separately (no interactions), we shall only consider one of them, as depicted in Figure 1. The three superheaters are labeled LTS, MTS and HTS, respectively for Low, Medium and High-Temperature Superheater. The input and output steam temperatures of MTS and HTS are measured and currently used in two cascade control structures, the goal being set-point control of the output temperatures of MTS and HTS. The four temperatures are labeled T_{in}^{MT}, T_{out}^{MT}, T_{in}^{HT} and T_{out}^{HT}. The output temperatures are controlled by means of an atemperator system based on water injection at the *inlet* of each superheater, in order to cool the steel pipes as well and preserve them from thermal stress and damage. The control of T_{out}^{HT} is also crucial for the safety of the turbine.

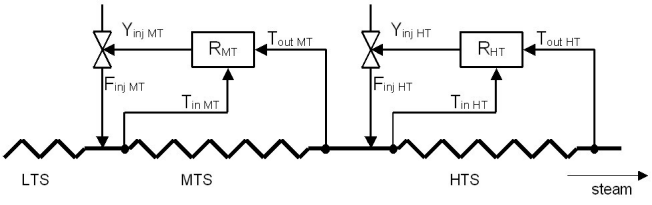

Figure 1: Superheaters and temperature control system

The controllers compute setpoints for the injection water flows respectively denoted F_{inj}^{MT} and F_{inj}^{HT}. They are con-

verted into valve position setpoints Y_{inj}^{MT} and Y_{inj}^{HT} via look-up tables representing the inverted valves characteristics, and possible flow controllers in case the inversion of the static nonlinearities only is not satisfactory. These possible flow controllers as well as the valves controllers (positioners) are considered as part of the process.

3 Control objective

3.1 Technical aspects

In order to achieve better performance during important transients (load changes, pressure variations due to primary frequency control, etc.), the current cascade PID controllers will be replaced by Linear Quadratic Gaussian controllers based on black-box models identified at several operating points. The goal is to reduce the standard deviations of T_{out}^{MT} and T_{out}^{HT} as well as their overshoot peak values during these transients, or to increase the speed at which load changes can be done while keeping the temperatures in the same ranges as with the PID controllers if those are already satisfactory.

3.2 Economic interpretation

The economics of steam temperature standard deviation reduction are illustrated in Figure 2.

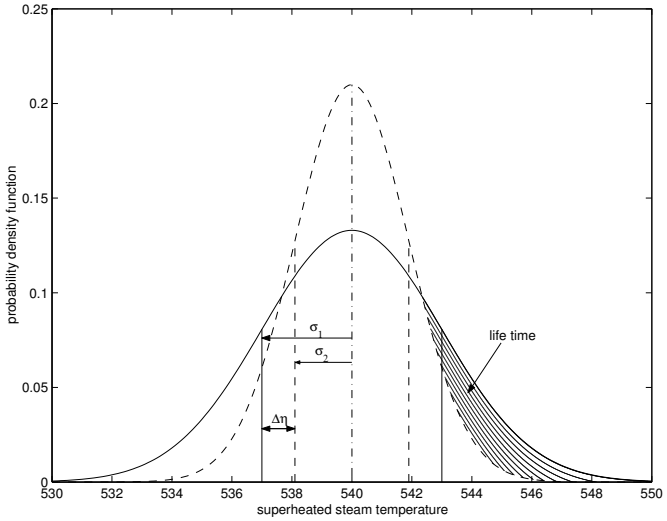

Figure 2: Steam temperature PDF with suboptimal controller (—) and optimal controller (−−)

A first issue concerns the life time of the superheaters. The wear undergone by the steel depends highly on the temperature. Excessive temperatures have a cumulative negative effect on its life time. As a result, since the vertical axis of the probability density function is a normalised time axis, the shaded surface between the two curves is representative of the life time that can be saved by reducing the temperature standard deviation.

A second issue is the influence of the steam temperature on the thermal efficiency η of the plant. A higher temperature means a higher enthalpy hence a more efficient expansion in the turbine and more power produced for the same fuel consumption. For superheated steam at 125 bar and 540°C, the expansion efficiency of the high-pressure turbine, which is defined as the ratio between the actual shaft work and the maximum shaft work that would be produced by an ideal isentropic expansion, is 74.57% (assuming outlet steam pressure and temperature of 28 bar and 350°C). A drop of 4°C at the inlet of the turbine, causing a drop of about 2°C at the outlet, would yield an expansion efficiency of 73.77%. The difference may seem negligible, but for a 300 MW plant it represents a loss of more or less 1.25 MW. Of course, positive deviations of the temperature have a positive effect on the plant efficiency, but this is counterbalanced by the life time reduction it causes. The same exercise could be done for the reheated steam temperature which influences the low-pressure turbine efficiency.

As a result, the best solution is to work at a temperature setpoint that is as close as possible to the maximum value admissible by the material, considering the temperature standard deviation which has to be as small as possible.

4 Control design

4.1 Control structure

Because there is no backwards influence from the HTS to the MTS, a separate controller can be designed for each superheater without loosing any degree of freedom.

The fuel flow F_{fuel} and the high-pressure turbine inlet valve aperture Y_{HP} have got a major influence on the steam temperature; since they are measured, they can be used by the new LQG controllers in a feed-forward way (in fact, they will be used as inputs to the Kalman state estimators). As T_{out}^{MT} strongly influences the temperature in the HTS downstream, it will also be used in a feed-forward way by the LQG controller for T_{out}^{HT}. Finally, T_{in}^{MT} and T_{in}^{HT} will be measured and used by the controllers, but not controlled. Their variations will indeed propagate to T_{out}^{MT} and T_{out}^{HT} with a slow time constant, hence it is useful to measure and use them. They may however be subject to disturbances opposite to those directly affecting T_{out}^{MT} and T_{out}^{HT}, yielding a potentially conflictual control problem if they were to be controlled as well (the occurrence of such opposite disturbances can dramatically impair the performance of standard cascade control loops where input temperature control is used as an intermediate step for output temperature control).

4.2 Model structure

For reasons of objectivity, the simulator is considered as a black-box process and measured data are used to identify all the transfer functions that will be used by the

controllers. In accordance with the control structure described above, the following model structure is chosen:

$$\begin{bmatrix} T_{in}^{MT} \\ T_{out}^{MT} \end{bmatrix} = \underbrace{\begin{bmatrix} G_1 & H_1 & 1 & 0 & P_1 \\ G_2 & H_2 & P_2 & 1 & P_2P_1 \end{bmatrix}}_{S^{MT}(s)} \begin{bmatrix} F_{fuel} \\ Y_{HP} \\ \Delta T_{in}^{MT} \\ \Delta T_{out}^{MT} \\ F_{inj}^{MT} \end{bmatrix}; \quad (1a)$$

$$\begin{bmatrix} T_{in}^{HT} \\ T_{out}^{HT} \end{bmatrix} = \underbrace{\begin{bmatrix} P_3 & G_3 & H_3 & 1 & 0 & P_4 \\ P_5P_3 & G_4 & H_4 & P_5 & 1 & P_5P_4 \end{bmatrix}}_{S^{HT}(s)} \begin{bmatrix} T_{out}^{MT} \\ F_{fuel} \\ Y_{HP} \\ \Delta T_{in}^{HT} \\ \Delta T_{out}^{HT} \\ F_{inj}^{HT} \end{bmatrix}. \quad (1b)$$

Here, $\Delta T_{in/out}^{MT/HT}$ represent unmeasured temperature disturbances. It is a convenient way of modelling all disturbances that do not come from F_{fuel} or Y_{HP}.

4.3 Identification procedure

For the MTS (resp. the HTS), P_1 and P_2 (resp. P_4 and P_5) are identified using closed-loop data. The excitation signal is a PRBS applied to the setpoint of T_{out}^{MT} (resp. that of T_{out}^{HT}). The controllers used during indentification are the *optimised* cascade PID controllers we want to replace. The reasons for performing the identification in closed loop, which may seem a rather eccentric approach in comparison to common industrial practice, are motivated by recent scientific results on identification and modelling for control [2, 5, 6, 7, 10]. The essential message they carry is the fact that *identification in closed loop with a controller as close as possible to the optimal (yet to be designed) one, delivers models with errors that are ideally tuned for control design.* Putting it simply, the model will be very precise at frequencies that are important from a closed-loop point of view (essentially around the cross-over frequency of the system, where the stability margins are determined) and possibly more sloppy at frequencies that are less important, contrary to open-loop identification which would deliver a model with an average and uniformly distributed error[1].

The other transfer functions are identified using open-loop data. Indeed, these are transfer functions between exogenous signals (measured disturbances) and the outputs of the system. Closing the loop would prevent us from correctly identifiying them; instead, we would identify the closed-loop sensitivity functions to these disturbances.

This identification procedure is repeated at several load values: 280 MW, 220 MW, 190 MW and 130 MW.

[1]To evidence this, we also identified models from open-loop data and we used them to compute LQG controllers as we did with those identified in closed loop. To do this, we applied PRBS's directly to Y_{inj}^{MT} and Y_{inj}^{HT}; their variances were chosen such as to produce the same temperatures amplitudes as during closed-loop identification. Although very good and similar *nominal* performance were achieved in both cases (i.e. when connecting the controllers to the corresponding identified models), the controllers based on open-loop models actually destabilised the process (i.e. the simulator) while those based on closed-loop models proved to be very satisfactory as we shall see further.

4.4 Principles of LQG

Here we briefly recall the principles of Linear Quadratic Gaussian control design with loop shaping [1] before applying them to the models described in (1).

Let us consider a linear time-invariant plant model

$$\mathcal{M}: \quad \begin{bmatrix} z(t) \\ y(t) \end{bmatrix} = S(s) \begin{bmatrix} p(t) \\ v(t) \\ u(t) \end{bmatrix} \quad (2)$$

where y, z, p, v and u are column vectors containing respectively the controlled outputs, the measured but uncontrolled outputs, the measured disturbances, the unmeasured disturbances and the control inputs of S.

The control design consists of the following steps.

1. *Loop shaping*: In order to emphasise those frequencies where the control action should be enhanced, a loop-shaping filter $L(s)$ can be used. The shaped plant is $\tilde{S}(s) = L(s)S(s)$. Normally a bloc-diagonal structure is used for $L(s)$: $L(s) = \begin{bmatrix} L_z(s) & 0 \\ 0 & L_y(s) \end{bmatrix}$. $L_y(s)$ will generally contain an integrator in order to ensure zero static error, while $L_z(s)$ will most of the time be the identity matrix. The controller is then designed for the shaped plant $\tilde{S}(s)$.

2. *State feedback gain computation*: A static state feedback gain matrix K : $u(t) = Kx(t)$ (where $x(t)$ is the state vector of $\tilde{S}$) is computed such as to minimise the following cost function:

$$J_{LQG} = \int_0^\infty \Big(\Big[L_y(s)y(t) \Big]^T Q \Big[L_y(s)y(t) \Big] + u^T(t) R u(t) \Big) dt. \quad (3)$$

   In this cost function, Q and R are positive-definite matrices aimed at putting more weight on some outputs or more penalty on some inputs. Computing K requires solving a Ricatti equation based on the state matrices of $\tilde{S}$ and on Q and R.

3. *Kalman filter design*: Because the state $x(t)$ of the shaped system $\tilde{S}$ is normally unknown, one has to build an estimate $\hat{x}(t)$ of it in order to implement the feedback law as $u(t) = K\hat{x}(t)$. This estimate is obtained by means of a Kalman filter which takes as inputs all relevant measured input and output signals of the shaped plant, namely $L_y(s)y(t)$, $L_z(s)z(t)$, $p(t)$ and $u(t)$. The Kalman filter state equations contain a gain matrix which is also the solution of a Ricatti equation depending on the state matrices of $\tilde{S}$ and on the covariance matrices Q_v and R_n of the unmeasured disturbances and of the measurement noise, respectively. In practice, these two matrices are used freely by the designer as tuning parameters.

4. *Controller implementation*: The complete controller is obtained by connecting the gain matrix K and the Kalman filter together as depicted in Figure 3. Because the controller was designed for the shaped system $\tilde{S}$, the filter $L(s)$ must be added to it before it can be used with the initial system S.

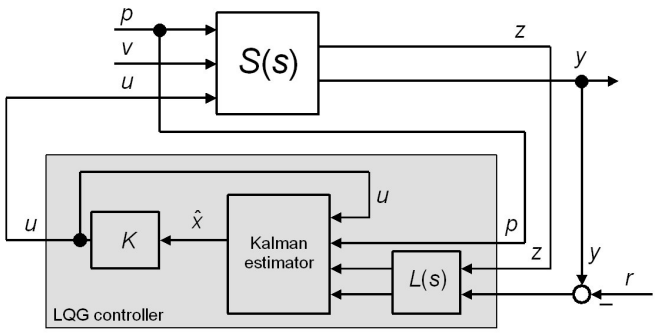

Figure 3: LQG controller with loop-shaping filter

4.5 Application to the superheaters

Since each superheater has got only one control input and one controlled output, the weightings Q and R in (3) are scalar and can be replaced by their ratio λ. The control design objective then becomes the minimisation of the following loss function for each superheater:

$$J^i_{LQG} = \int_0^\infty \left(\left(L^i_y(s) T^i_{out}(t)\right)^2 + \lambda^i \left(F^i_{inj}(t)\right)^2 \right) dt, \quad (4)$$

where i is either MT or HT.

The computation of the controller is carried out as explained above. The following remarks can be made about the tuning parameters:

- In the present application, an integrator in series with a lead-lag filter proved very satisfactory for $L^i_y(s)$;
- λ^i equally penalises the control action at all frequencies, but its effect is only perceivable at frequencies where $|L^i_y(e^{j\omega})|$ is small, i.e. essentially at high frequencies. A large λ^i yields more robust controllers, less actuator wear, but also poorer performance;
- Q^i_v and R^i_n are 2×2 matrices. They are the covariance matrices of the unmeasured disturbances $\begin{bmatrix}\Delta T^i_{in} & \Delta T^i_{out}\end{bmatrix}^T$ and of the measurement noise on $\begin{bmatrix}T^i_{in} & T^i_{out}\end{bmatrix}^T$. They can be chosen diagonal if we assume no correlation neither between disturbances on the input and output temperatures, nor between their respective measurement noises.

4.6 Dealing with plant nonlinearities

LQG controllers are designed for each of the 280 MW, 220 MW, 190 MW and 130 MW load values. Linear interpolation between the outputs of two adjacent controllers is then used to compute the control signals at intermediate loads. Controllers which are not used at a specific load must be switched off. On/off switchings are carried out bumpless thanks to the programming of an appropriate state initialisation procedure.

Because Cogito NT does not allow the programming of complex transfer functions, the LQG controllers are programmed and run in Simulink. The connection between both systems is done via an OPC interface.

5 Simulation results

5.1 Performance during load change

The first test we carried out is a load change from 130 MW to 285 MW with a slope of 6 MW/min. During this test, the superheated steam absolute pressure changed from 81 bar to 126.5 bar. The setpoints for T^{MT}_{out} and T^{HT}_{out} were 456°C and 540°C, respectively. Figure 4 shows the measurements of both temperatures during the test, as well as those of the valves positions Y^{MT}_{inj} and Y^{HT}_{inj}, the load, the steam pressure, the fuel flow F_{fuel} and the high-pressure turbine inlet valve aperture Y_{HP}. Qualitatively, the new LQG controllers outperform the optimised PID controllers (which are also adapted in function of the load).

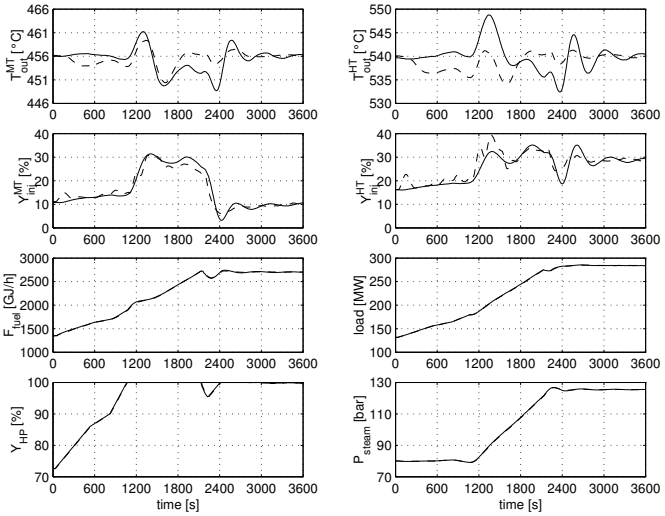

Figure 4: 6 MW/min load change with PID (—) and LQG (−−)

This observation is confirmed by the figures presented in Table 1[2]: the standard deviations of T^{HT}_{out} was reduced by 34% and, more importantly, its overshoot peak value decreased by 85%[3]. Since this overshoot is often the stumbling block that prevents faster load changes, this is a remarkable result. Of course, these improvements have got a price: more nervous control action, hence more actuator

[2] Due to space limitation, we only present numerical results for T^{HT}_{out}. Those for T^{MT}_{out} are similar.

[3] The overshoot and undershoot peaks are respectively caused by changes in $\dot{Y}_{HP}$ and $\dot{F}_{fuel}$, which explains their asymmetry.

wear, as the standard deviation of the valve speed $\dot{Y}_{inj}^{HT}$ shows. The histograms of Figure 5 show however that the additionnal actuator wear is not excessive in comparison with the improvement of the temperature profile.

	PID	LQG	improv.
standard deviation of T_{out}^{HT}	2.9°C	1.9°C	34%
overshoot peak of T_{out}^{HT}	8.8°C	1.3°C	85%
undershoot peak of T_{out}^{HT}	-7.6°C	-5.9°C	22%
standard deviation of $\dot{Y}_{inj}^{HT}$	0.035%/s	0.046%/s	-31%

Table 1: 6 MW/min load change with PID and LQG

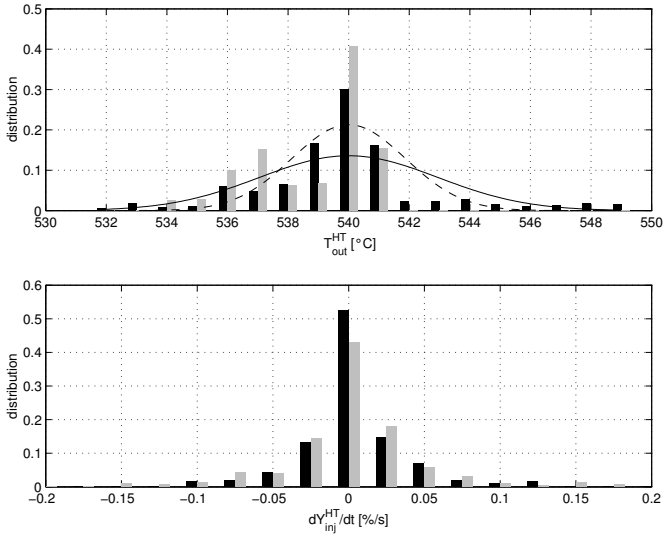

Figure 5: 6 MW/min load change: histograms and Gaussian fits with PID (black, —) and LQG (gray, −−)

5.2 Load change with increased gradient

A second test we have carried out is to increase the slope of the load change. We found that LQG made it possible to increase it by 33% (8 MW/min instead of 6 MW/min) without causing more thermal stress than PID at 6 MW/min. This is shown in Figure 6 and in Table 2. Here, the limitations come from increased actuator wear and larger (yet acceptable) temperature undershoot.

5.3 Performance during grid frequency control

When a power plant takes part to the electrical grid frequency primary control, the high-pressure turbine inlet valve is modulated by the variations of this frequency while the steam pressure is controlled by the boiler's principal controller which acts on the fuel flow. These two actions have a very disturbing effect on the steam temperature. When an important incident occurs (typically a frequency drop of several tens of mHz), this results in a stepwise sollicitation of the turbine valve. Accordingly, the third test we carried out is the application of 10% steps to Y_{HP}. The results are presented in Figures 7 and 8 and in Table 3. In this case, the LQG controllers have a positive effect on the temperatures oscillations by reducing their amplitudes and settling times, which is also healthy for the injection valves: they spend more time at rest than with PID controllers.

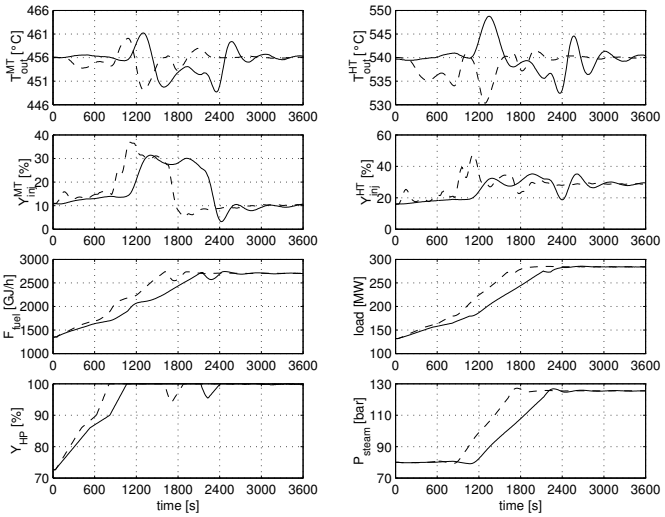

Figure 6: Load change with PID at 6 MW/min (—) and LQG at 8 MW/min (−−)

	PID	LQG	improv.
standard deviation of T_{out}^{HT}	2.9°C	2.5°C	14%
overshoot peak of T_{out}^{HT}	8.8°C	1.6°C	82%
undershoot peak of T_{out}^{HT}	-7.6°C	-9.7°C	-27%
standard deviation of $\dot{Y}_{inj}^{HT}$	0.035%/s	0.066%/s	-89%

Table 2: Load change with PID at 6 MW/min and LQG at 8 MW/min

	PID	LQG	improv.
standard deviation of T_{out}^{HT}	1.9°C	0.8°C	58%
overshoot peak of T_{out}^{HT}	5.9°C	3.7°C	37%
undershoot peak of T_{out}^{HT}	-5.5°C	-3.3°C	40%
mean 1°C settling time of T_{out}^{HT}	1002 s	333 s	67%

Table 3: Temperature regulation during frequency control

5.4 Economic interpretation

Tables 1 and 3 show that the improvement of the standard deviation σ of T_{out}^{HT} is about 1°C with LQG controllers, as well during load changes as during nominal plant operation with grid frequency control. Hence, in order to keep the temperature with PID controllers 99% of the time under the same limit as with LQG controllers, the setpoint of T_{out}^{HT} would have to be reduced to $540°C - 2.4 \times (\sigma_{PID} - \sigma_{LQG}) \approx 537.6°C$ when the PID controllers are used. At full load, this would represent a loss of shaft work of 3.4 kJ/kg as shown in Table 4. For a

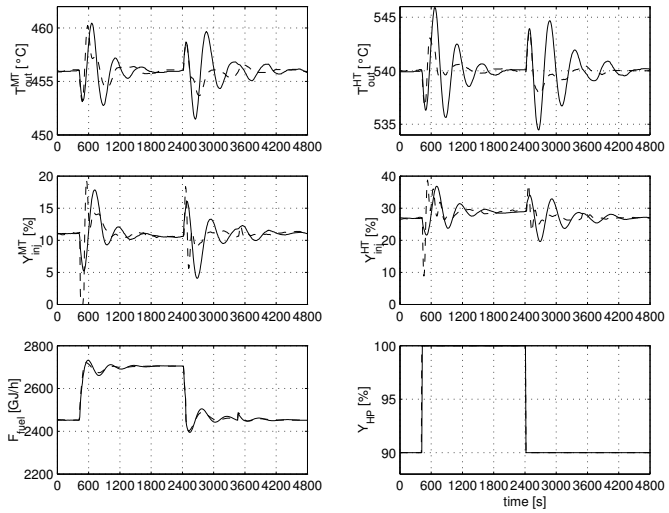

Figure 7: Temperature regulation with PID (—) and LQG (−−) during grid frequency control

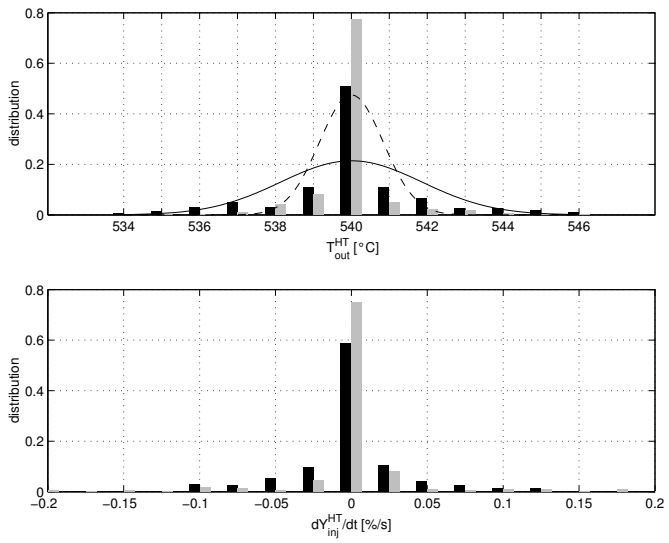

Figure 8: Histograms and gaussian fits with PID (black, —) and LQG (gray, −−) during grid frequency control

plant working 8000 hours a year at full load (steam flow of 800 t/h), the yearly production loss $\Delta\mathcal{E}$ would be

$$\Delta\mathcal{P} = 3.4 \text{ kJ/kg} \times 800 \text{ t/h} = 0.75 \text{ MW}, \quad (5a)$$

$$\Delta\mathcal{E} = \Delta\mathcal{P} \times 8000 \text{ h/year} = 6000 \text{ MWh/year}. \quad (5b)$$

In these computations, we have only considered the loss of efficiency of the high-pressure turbine (the low-pressure turbine is not represented in our simulator). Actually, it is our experience that the same problem is likely to occur with the reheated steam temperature, which would yield a total power loss $\Delta\mathcal{P} \approx 1.5$ MW. Also, we have only treated the problem from the probabilistic side but, in practice, peak values are also an issue because of the incurred risk of material damage. In the present situation,

	inlet	outlet	work (Δh)
LQG	T=540°C	T=350°C	
	P=126.5 bar	P=28 bar	
	h=3446.0 kJ/kg	h=3118.9 kJ/kg	327.1 kJ/kg
PID	T=537.6°C	T=348.8°C	
	P=126.5 bar	P=28 bar	
	h=3439.7 kJ/kg	h=3116.0 kJ/kg	323.7 kJ/kg
difference			3.4 kJ/kg

Table 4: Effect of steam temperature setpoint reduction with PID controllers

the overshoot peak value for T_{out}^{HT} during load change is 8.8°C with PID controllers; an operator concerned by this safety issue might decide to reduce the temperature setpoint by 4 or 5°C, yielding further efficiency loss.

6 Conclusion

We have investigated the advantages of a modern advanced control method, namely Linear Quadratic Gaussian control, over optimised PID controllers for steam temperature regulation in a power plant boiler. The analysis of our results shows that LQG outperforms PID in terms of control performance, and that this control improvement has got a significant economic impact by virtue of extended material life time and increased turbine efficiency.

References

[1] B.D.O. Anderson and J.B. Moore. *Optimal Control: Linear Quadratic Methods*. Prentice-Hall, Englewood Cliffs, New Jersey, USA, 1989.

[2] B. Codrons. *Experiment Design Issues in Modelling for Control*. PhD thesis, Université Catholique de Louvain, Louvain-la-Neuve, Belgium, 2000.

[3] B. Codrons, H. Demaret, and J.-C. Lemoine. Simulator for thermal power plants and the network they supply. *Journal A*, 43(2):15–16, 2002. Feature issue on simulators for operator training.

[4] R. Cori and C. Maffezzoni. Practical optimal control of a drum boiler power plant. *Automatica*, 20:163–173, 1984.

[5] M. Gevers. Towards a joint design of identification and control? In H.L. Trentelman and J.C. Willems, editors, *Essays on Control: Perspectives in the Theory and its Applications*, pages 111–151. Birkhauser, New York, USA, 1993.

[6] M. Gevers, B.D.O. Anderson, and B. Codrons. Issues in modeling for control. In *Proc. of the 1998 American Control Conference*, pages 1615–1619, Philadelphia, Pennsylvania, USA, 1998.

[7] H. Hjalmarsson, M. Gevers, and F. De Bruyne. For model-based control design, closed-loop identification gives better performance. *Automatica*, 32:1659–1673, 1996.

[8] G. Prasad, G.W. Irwin, E. Swindenbank, and B.W. Hogg. A novel hierarchical approach to plant-wide control of a thermal power unit. In *Proc. of the IFAC Symposium on Power Plants and Power Systems Control*, pages 449–455, Brussels, Belgium, 2000.

[9] W. Tan, H.J. Marquez, and T. Chen. Multivariable robust controller design for a boiler system. *IEEE Trans. on Control System Technology*, 10(5):735–742, 2002.

[10] P.M.J. Van den Hof and R.J.P. Schrama. Identification and control – closed-loop issues. *Automatica*, 31:1751–1770, 1995.